Instantaneous Rotational Speed Measurement of Wind Turbine Blades using a Marker-Tracking Method

Yi-Hsiang Liao
School of Engineering
University of Kent
Canterbury, United Kingdom
yl370@kent.ac.uk

Lijuan Wang
School of Engineering
University of Kent
Canterbury, United Kingdom
l.wang@kent.ac.uk

Yong Yan
School of Engineering
University of Kent
Canterbury, United Kingdom
y.yan@kent.ac.uk

***Abstract*—Rotational speed of wind turbine blades is an important parameter reflecting the operating and structural health conditions of wind turbines. Traditionally, the rotor speed is measured using inertial measuring units (IMUs). The biggest issue with IMUs is that the measurements drift over time and require constant calibration. This paper presents a direct way of measuring the instantaneous rotational speed of wind turbine blades using a camera and a marker-tracking method. The proposed measurement method is assessed by conducting a series of simulation experiments under different conditions – fixed speed, stepped varying speed, and linear varying speed. Results demonstrate that when using a camera with a frame rate of 30 fps (frames per second), the marker-tracking method yields a relative error within ±0.5% at the speed between 5 to 30 rpm (revolutions per minute). Compared to the image-correlation method, the marker-tracking method provides better results in terms of accuracy and reaction time, especially under varying speed conditions.**

Keywords—rotational speed measurement, wind turbine blade speed, image correlation, marker tracking, instantaneous speed measurement

I. Introduction

The rotational speed of wind turbine blades is one of the parameters recorded for condition monitoring. This is because the rotational speed of blades is related not only to the wind turbines' performance but also to their structural health. Therefore, accurate and real-time measurement of instantaneous speed of wind turbine blades is helpful to detect potential faults in advance and prevent major failures, thus reducing the downtime of wind turbines and decreasing maintenance costs [1].

The rotational speed of rotating machinery has been traditionally measured using tachometers. Several types of tachometers were developed for various applications, based on different working principles. A common type is a mechanical tachometer, which requires to be physically connected to the rotating object being measured. Although mechanical tachometers can provide accurate results, their major drawback is that the contact points such as connected surfaces, belts, or joints may wear off over time. As a result, mechanical tachometers require regular monitoring and maintenance. For this reason, several non-contact tachometers were invented, such as magnetic sensors [2], [3], which can be used to encode a rotating machine's angular position and rotational speed without contact, wear and tear. Another way of measuring rotational speed using electrostatic sensors is proposed in recent years [4], [5]. However, this type of sensor does not apply to measuring the rotational speed of wind turbines due to the lack of electrostatic charges generated from the slow rotation. The most widely adopted type of tachometer is the optical tachometer. Optical tachometers work by emitting a light source and a photosensor receiving the reflected light from a marker. The measurement is taken by counting the period of the reflection. They are widely adopted in the industry due to their mature technology and reliability. Nevertheless, this method is unsuitable for wind turbine applications because wind turbine blades are very far apart.

With the advancement of image processing techniques, a new type of speed measurement instrument has appeared – video tachometers. Video tachometers use video tracking methods to find changes in adjacent frames in order to measure direction and speed. Guo et el. [6] used a variation of the Lucas-Kanade method [7] for video tracking to measure a simple shaft with a random pattern. Moreover, another kind of video tachometer uses image correlation to get a periodic similarity signal and then applies frequency analysis to measure the rotational frequency [8], [9]. Imaging methods have also been used to measure the rotor speed of wind turbines. Ozbek et al. [10] did a pioneering study using photogrammetry to track retroreflectors in order to measure the speed of the wind turbine blades. However, this method requires specific lighting conditions. It is mentioned in their paper that the data collection can only be performed around sunset so that the retroreflectors are bright enough for the cameras to pick up [10]. In addition, recently, Natili et al. [1] analyzed the frequency response of image correlation values. Although this method has proven robust and produces accurate results, it relies on precisely tuned parameters and many padded zeros used in the image correlation algorithm.

This research presents a marker-tracking method for measuring the instantaneous speed of wind turbine blades using a low-cost imaging system. Compared to photogrammetry approaches, this non-contact measurement method requires almost no camera calibration and no specific lighting conditions. To evaluate the performance of the marker-tracking method, simulation experiments were carried out in different conditions including fixed speed, stepped variable speed and linear varying speed. Performance comparison between the marker-tracing method and the image-correlation method is conducted in terms of accuracy and reaction time.

II. METHODOLOGY

To measure the rotational speed of wind turbine blades, a camera is required aiming at the wind turbine hub perpendicular to the rotational plane. This can be done by mounting a camera onto a drone in real-life applications. In this paper, a marker-tracking method is proposed. It is then compared with the state-of-the-art image-correlation method. The marker-tracking method necessitates the use of markers. A marker is placed on each blade near the center of the rotor to ensure that three markers are all visible to the camera. The primary measurement processes are illustrated in Fig. 1. The images of the wind turbine blades are captured by the camera and then processed in two different ways. The marker-tracking method aims to calculate the rotation angle of each blade between two adjacent images and then convert the rotation angle to rotational speed, provided the frame rate is known. The image-correlation method aims to find the rotational frequency through image similarity evaluation and frequency analysis and then convert the rotational frequency to rotational speed.

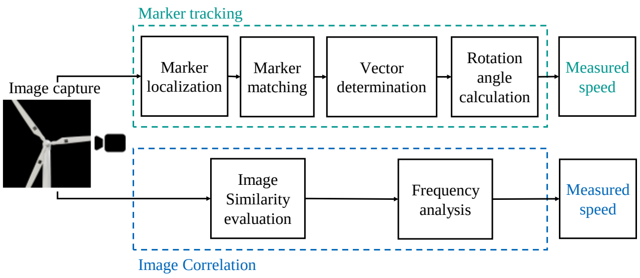

Fig. 1. General measurement process.

A. Marker-Tracking based Rotational Speed Measurement

The marker-tracking method starts with marker localization. In this paper, a blob detector is used to find the center of each marker in an image. Fig. 2 shows the main steps of the blob detector. First, a single image (Fig. 2 (a)) acquired by the camera is converted into several binary images (Fig. 2 (b)) using different thresholds of grayscale levels. For each binary image, the contour is found based on the connectivity of the black or white patches. The centroid of each contour (Fig. 2 (c)) is then calculated using the image moments. Next, the radius of each patch is calculated based on the distance between the contour points and the centroid. Then, the centroids whose radii intersect are grouped. The final location of the marker (Fig. 2 (d)) is the mean of all the grouped centroid coordinates.

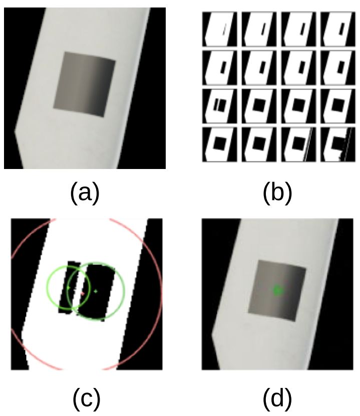

Fig. 2. Process of blob detection.

The marker matching process is to identify the same marker in the two adjacent frames. Markers are matched based on the shortest Euclidean pixel distance between markers' coordinates. For each marker, as shown in Fig. 3, the vector $\vec{v}_{i,j}$ is formed from the center of the rotation to the marker coordinate; with $i \in \{1, \ldots, 3\}$ as blade index and $j \in \{1, \ldots, k\}$ as the frame number. The rotation angle (θ_i) during the sampling interval is then calculated using the geometric definition of vector dot product according to (1).

$$\theta_i = \arccos \frac{\vec{v}_{i,j} \cdot \vec{v}_{i,j+1}}{|\vec{v}_{i,j}||\vec{v}_{i,j+1}|} \quad (1)$$

The rotational speed of each blade can be derived based on the rotation angle (θ_i). The final rotational speed N is the average of individual speeds and is represented as (2).

$$N = \frac{1}{3} \sum_{i=1}^{3} \frac{60 f_s}{2\pi} \theta_i \quad (2)$$

where f_s is the sampling frequency.

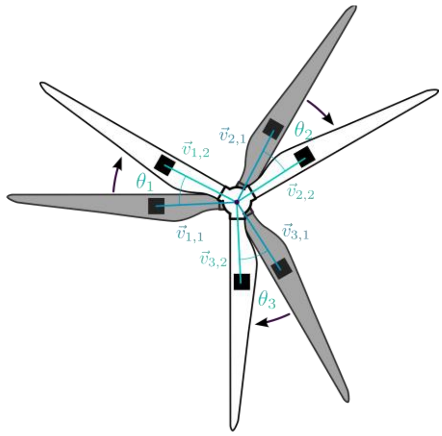

Fig. 3. Principle of the marker-tracking method (frame 1 blades in gray and frame 2 blades in white).

B . Image-Correlation based Rotational Speed Measurement

Image correlation is used to quantify the similarity level between two images. The first frame captured by the camera is taken as the reference image. The correlation coefficient (r) representing the similarity level between the reference image (X_{ij}) and the subsequent image (Y_{ij}) is calculated as:

$$r = \frac{\sum_{i=1}^{m} \sum_{j=1}^{n} [X_{ij} - \overline{X}][Y_{ij} - \overline{Y}]}{\sqrt{\sum_{i=1}^{m} \sum_{j=1}^{n} [X_{ij} - \overline{X}]^2 \cdot \sum_{i=1}^{m} \sum_{j=1}^{n} [Y_{ij} - \overline{Y}]^2}} \quad (3)$$

where the image size is $m \times n$. The indices i, j are the row and column index of the image, respectively. The larger the correlation coefficient, the higher the similarity level between the reference image and the subsequent image. Due to the rotational motion of the wind turbine and continuous processing of images, the similarity level of sequential images can be regarded as a periodic signal. Since the three blades of the wind turbine are symmetric with the hub, the frequency of the similarity signal is three times the rotational frequency.

In order to find the dominant frequency of the similarity signal, the short-time Fourier transform (STFT) is applied. STFT works by slicing the signal into small sections using a temporal sliding window and applying Fast Fourier Transform (FFT) onto each section. It is worth noting that the sliding window size must include at least one period of the similarity signal; otherwise, the determination of the dominant frequency would be negatively affected, thus leading to false measurement results.

The obtained dominant frequency (f) from STFT can then be converted to rotational speed using (4).

$$\mathrm{N} = \frac{60f}{3} = 20f \tag{4}$$

III. Results and Discussion

A simulation was set up using 3D animation software to simulate a wind turbine rotating under different speed conditions. The most significant benefit of using animation software is the ability to change conditions with ease. Environmental conditions such as lighting, background, camera position, and test conditions like varying speeds can be applied through scripting.

A. *Simulation Setup*

The simulation was created using Blender 2.93, an open-source 3D computer graphics software. As shown in Fig. 4, the simulated wind turbine model is developed based on a real wind turbine - Nordtank NTK 300. It has a tower height of 35 meters and a blade length of 31 meters. The black square marker on each blade is 0.8 meters wide and is placed 4 meters away from the center of the hub. The whole scene is lit by a high dynamic range image (HDRI) to give it a natural lighting condition. In addition, another sun lamp is placed at the same angle as the sun position on the HDRI. The angle of the sun lamp is 38 degrees from the front of the modeled turbine.

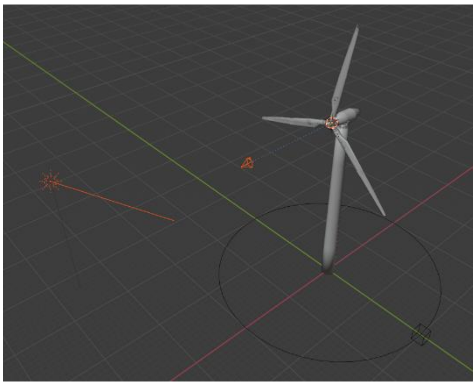

Fig. 4. Simulation environment

During the simulation experiment, the camera was placed 20 meters away from the hub, perpendicular to the plane of rotation, filming at 30 frames per second (fps). The resulting image dimension is 720×720 pixels. There are no distortions since a pinhole camera is used, and camera calibration is unnecessary.

The following three conditions were simulated in order to obtain the images of wind turbines rotating in a variety of scenarios:

- Fixed speed. From 5 rpm to 30 rpm in 2.5 rpm intervals. Each speed has 10 seconds of footage.
- Stepped varying speed. A single sequence from 5 rpm to 30 rpm in 5 rpm intervals.
- Linear varying speed. Starting from 5 to 30 rpm in a 20-second interval.

These conditions are calculated using Newtonian motion equations and then fed into the blender's animation system through key-frames. The rotation position of the modeled wind turbine is accurately simulated at each sampling frame.

B. *Test Results*

1) Fixed Speed Results: The marker-tracking and image-correlation rotational speed measurement methods were tested under a series of fixed speeds from 5 rpm to 30 rpm. Fig. 5 shows the calculated rotational speed using the two methods under the speed condition of 5 rpm. With the recording time of 10 seconds and the sampling rate of 30 fps, the render resulted in 300 frames for image processing. The marker-tracking rotational speed measurement method calculates the rotation angle between any two adjacent frames and produces a rotational speed value. Therefore, 299 calculated speed values were obtained from the marker-tracking method during the 10 second period. However, the calculated rotational speed from the image-correlation method depends on the window size used in STFT algorithm. Three different window sizes (80, 120 and 200) are applied to the STFT algorithm, respectively, and the calculated speed results are depicted in Fig. 5. It can be seen that the smaller the window size the more calculated results can be obtained. However, the calculated speed with a smaller window size is fluctuating around the reference speed. When the window size is set to 200, only three calculated speeds are obtained from the image-correlation method but they are consistently close to the reference speed.

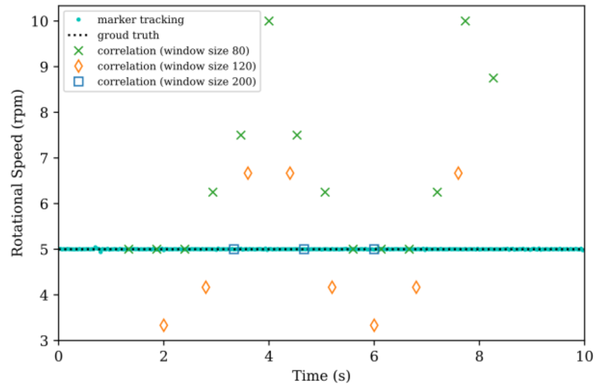

Fig. 5. Caluculated rotational speed with reference of 5 rpm.

In this study relative error is used to evaluate the accuracy of both methods. Fig. 6 shows the relative error of the calculated results under various fixed speed conditions using the marker-tracking method. The circle at each data point indicates the mean of the errors whereas the error bars indicate the maximum and minimum errors. It can be observed that the relative error at lower rotational speeds is slightly higher than higher rotational speeds. The highest error (-1.24%) occurs at 5 rpm. However, the relative error above 15 rpm is within ±0.5%.

The relative error of the calculated speed using the image-correlation method is shown in Fig. 7. It is clearly shown that the smaller the window size, the larger the error at lower rotational speeds. This is because with the same window size, lower rotational speeds yield less cycles and hence uncertainty in the determination of the rotational frequency. With the speed increased to 20 rpm or above, the relative error is reduced to 0.

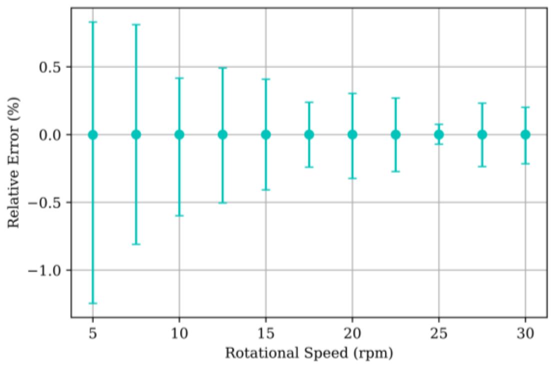

Fig. 6. Relative error of calculated results using marker-tracking method under fixed speed conditions.

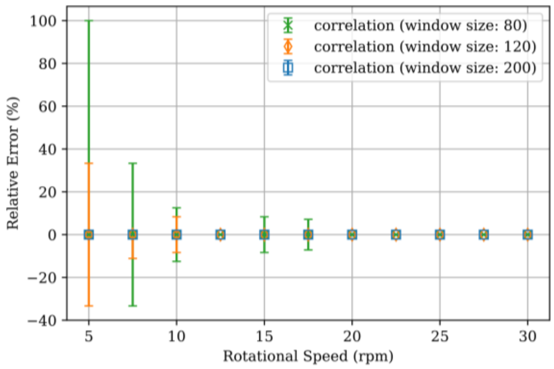

Fig. 7. Relative error of calculated results using image-correlation method under fixed speed conditions.

The marker-tracking method shows an increased error at lower rotational speeds due to reduced spatial resolution. Lower speeds are equivalent to smaller difference angles, which means that the deviation in marker coordinates will have a more significant effect on the result. The trade-off for the image-correlation method's high accuracy is its reaction time. With three speed values in 10 seconds, it can hardly be considered as real-time measurement.

2) Stepped Varying Speed Results: Fig. 8 shows the calculated results using the marker-tracking method, which can adapt quickly to the sharp rises of the steps. On the other hand, the image-correlation method can only produce three calculated results scattered along the way when the window size in the STFT algorithm is set to 200.

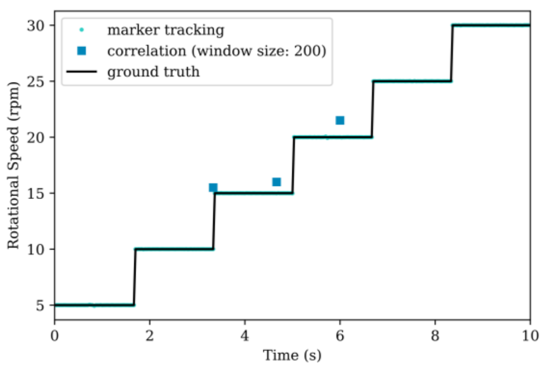

Fig. 8. Calculated results under stepped varying speed conditions.

The relative error of the calculated speed under stepped varying speed condition using the marker-tracking method is shown in Fig. 9. It clearly shows a similar trend with the fixed speed measurements. Most relative error values lie between ±0.5%, and only two calculated values are outside the range. These sudden errors are due to the blob detector detecting a shadow around the hub as a fourth marker. Due to the matching strategy of pixel distance, those markers were mismatched, thus creating a periodic error surge. However, as shown in Fig. 10, the maximum relative error of the calculated speed drived from the image-correlation method is more than 50%.

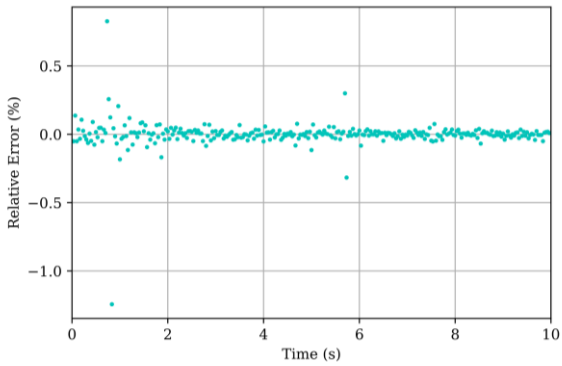

Fig. 9. Relative error of calculated results using marker-tracking method under stepped varying speed conditions.

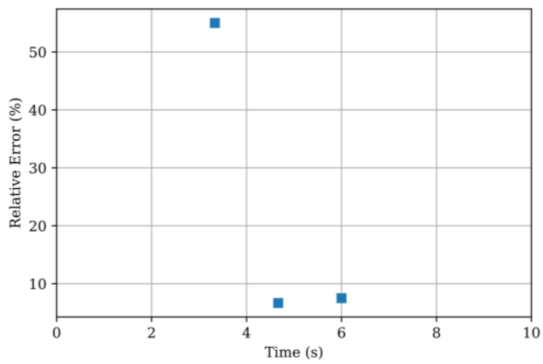

Fig. 10. Relative error of calculated results using image-correlation method under stepped varying speed conditions.

From the calculated results and the error analysis, it can be observed that the marker-tracking method is capable of producing accurate speed with a fast reaction time to stepped varing speed. The image-correlation method is unable to correctly determine the rotational frequency due to the sudden change in the speed and hence poor meeasurement accuracy.

3) Linear Varying Speed Results: Fig. 11 shows the rotational speed from the marker-tracking method when the speed is linearly increased from 5 rpm to 20 rpm. This proves that the method is effective for instantaneous rotational speed measurements. The image-correlation method is not compared in this scenario because the varying linear speed does not produce periodic correlation values, thus STFT is unable to find the pattern. As shown in Fig. 12, the relative error of the calculated results is within ±0.25% in most cases and maximum relative error is -1.04%.

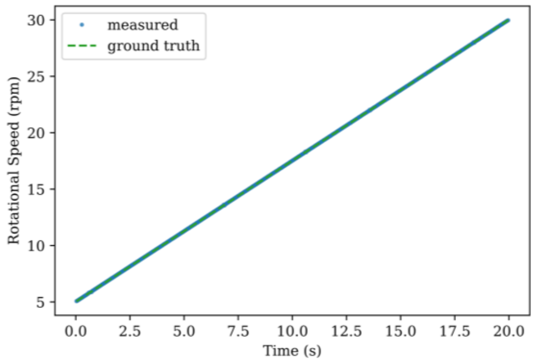

Fig. 11. Calculated results using marker-tracking method under linear varying speed conditions.

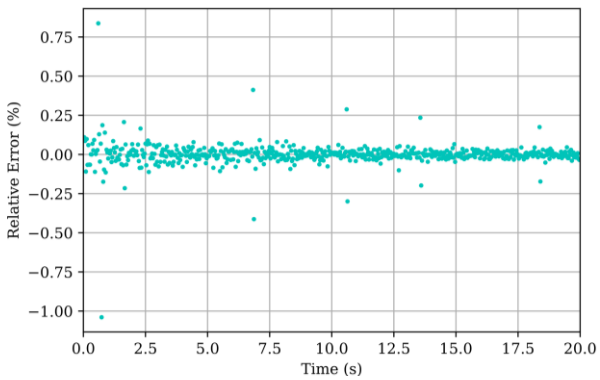

Fig. 12. Relative error of calculated results using marker-tracking method under varying linear speed conditions.

IV. Conclusion

In this paper, a marker-tracking method is proposed for measuring the instantaneous rotational speed of wind turbine blades. Simulation experiments were conducted to test the proposed method under various speed conditions such as fixed speed, stepped varying speed and linear varying speed. The relative error of the rotational speed obtained from the marker-tracking method is mostly between ±0.5%, with some random errors just above 1% in the measuring range of 5 - 30 rpm. This is due to the mismatch of markers in adjacent frames. The most important advantage of this method is that a measured speed value can be obtained by processing only two adjacent frames. In comparison, the image-correlation method was evaluated under the same conditions. The performance of the image-correlation method depends significantly on the window size in STFT algorithm. With a larger window size, the image-correlation method can achieve a higher accuracy under a fixed speed at the cost of reaction time. Under varying speed conditions, the marker-tracking method outperforms the image-correlation method in terms of accuracy and reaction time. Investigations into the effect of camera position, angle, and image resolution on the measurement results will be conducted in future studies. Moreover, the proposed method will be assessed on a physical test rig. This also opens an opportunity for testing the effects of camera instability, such as vibration and sway.

References

[1] F. Natili, F. Castellani, D. Astolfi, and M. Becchetti, "Video-Tachometer Methodology for Wind Turbine Rotor Speed Measurement," *Sensors*, vol. 20, no. 24, p. 7314, Jan. 2020, doi: 10.3390/s20247314.

[2] S. J. Arif, Imdadullah, and M. S. Jamil Asghar, "Rotating magnetic field based instantaneous angular speed measurement of low speed rotating machines," in *Proceedings of International Conference on Multimedia, Signal Processing and Communication Technologies*, Aligarh, India, Dec. 2011, pp. 252–255. doi: 10.1109/MSPCT.2011.6150487.

[3] L. A. Francis and K. Poletkin, *Magnetic Sensors and Devices: Technologies and Applications*. CRC Press, 2017.

[4] L. Wang, Y. Yan, Y. Hu, and X. Qian, "Rotational Speed Measurement Through Electrostatic Sensing and Correlation Signal Processing," *IEEE Trans. Instrum. Meas.*, vol. 63, no. 5, pp. 1190–1199, May 2014, doi: 10.1109/TIM.2013.2292283.

[5] L. Li, X. Wang, H. Hu, and X. Yang, "Speed condition monitoring of rotating machinery using electrostatic method," in *Proceedings of International Conference on Sensing Technology (ICST)*, Dec. 2015, pp. 345–350. doi: 10.1109/ICSensT.2015.7438420.

[6] J. Guo, C. Zhu, S. Lu, D. Zhang, and C. Zhang, "Vision-based measurement for rotational speed by improving Lucas–Kanade template tracking algorithm," *Appl. Opt.*, vol. 55, no. 25, pp. 7186–7194, Sep. 2016, doi: 10.1364/AO.55.007186.

[7] B. D. Lucas and T. Kanade, "An iterative image registration technique with an application to stereo vision," in *Proceedings of the 7th international joint conference on Artificial intelligence - Volume 2*, Vancouver, BC, Canada, Aug. 1981, pp. 674–679.

[8] Y. Wang, L. Wang, and Y. Yan, "Rotational speed measurement through digital imaging and image processing," in *2017 IEEE International Instrumentation and Measurement Technology Conference (I2MTC)*, May 2017, pp. 1–6. doi: 10.1109/I2MTC.2017.7969697.

[9] T. Wang, Y. Yan, L. Wang, and Y. Hu, "Rotational Speed Measurement Through Image Similarity Evaluation and Spectral Analysis," *IEEE Access*, vol. 6, pp. 46718–46730, 2018, doi: 10.1109/ACCESS.2018.2866479.

[10] M. Ozbek, F. Meng, and D. J. Rixen, "Challenges in testing and monitoring the in-operation vibration characteristics of wind turbines," *Mech. Syst. Signal Process.*, vol. 41, no. 1, pp. 649–666, Dec. 2013, doi: 10.1016/j.ymssp.2013.07.023.